

Is it possible to detect gravitational waves with atom interferometers?

G. M. Tino ¹, F. Vetrano ²

February 22, 2007

Abstract

We investigate the possibility to use atom interferometers to detect gravitational waves. We discuss the interaction of gravitational waves with an atom interferometer and analyze possible schemes.

PACS: 03.75.Dg; 04.30.-w; 04.80.Nn; 95.55.Ym; 39.20.+q

1 Introduction

The direct detection of Gravitational Waves (GWs) is one of the most exciting scientific goals because it would improve our understanding of laws governing the universe and provide new means to observe it. The most sensitive detectors which are already operating, under construction or being planned are based on optical interferometers [1, 2, 3]. In most cases, however, the sensitivities are only marginally sufficient to detect the expected signals, detectors have large sizes ranging from a few km on the Earth (Virgo, LIGO) to millions of km in space (LISA) and the operating frequency ranges are limited. Therefore it is of great interest to investigate alternative schemes that can lead to a higher sensitivity, smaller sizes and extend the frequency range of the detectors.

In recent years, matter-wave interferometry with neutral atoms has undergone an impressive development due to the increasing ability to control the internal and external atomic degrees of freedom using laser manipulation methods [4, 5, 6, 7]. Atom Interferometers (AIs) are already competing with state-of-art optical interferometers in terms of sensitivity. This was demonstrated experimentally for gravity acceleration [8], gravity gradients [9], inertial and rotation effects [10, 11]. Other experiments, planned or presently in progress, to investigate properties of gravitational field by AI concern accurate measurements of

¹Dipartimento di Fisica and LENS-Università di Firenze, INFN-Sezione di Firenze, Polo Scientifico, 50019 Sesto Fiorentino, Italy - E-mail: guglielmo.tino@fi.infn.it

²Istituto di Fisica-Università di Urbino, INFN-Sezione di Firenze, 61029 Urbino, Italy - E-mail: vetrano@fis.uniurb.it

G [12, 13], test of the equivalence principle [14], detection of the Lense-Thirring effect [15], deviations from the $1/r^2$ Newtonian law for small distances [16].

In analogy to optical interferometers, in atom interferometers atomic wave packets are split and recombined giving rise to an interference signal. Different schemes can be used for splitting, reflecting and recombining the atoms. In a particular class of interferometers, which is the one relevant in this paper, the separation of the atoms is achieved by inducing a transition between internal states of the atoms by an electromagnetic field. The spatial separation in this case is induced by the momentum recoil and the internal and external states of the atoms become entangled. Another approach is to use material gratings. This raises however different problems, both conceptual and technical, such as the realization and handling of the required nano-structures and it will not be considered here.

In this paper, we discuss the possibility to use AI to detect gravitational waves. The interaction between matter waves and gravitational waves was already investigated in [17, 18, 19, 20]. Recently, due to the experimental advances, the interest was revived [21, 22, 23, 24, 25]. The aim of the present paper is to analyze possible schemes for interferometers using light fields as atom optics components. Compared to [25], where only the Linet-Tourrenc contribution is considered in the eikonal approximation, we take into account all the contributions in phase difference inside the interferometer.

The paper is organized as follows. In Sect. 2 we recall the ABCD formalism for matter waves and apply it to the calculation of phase shift in atom interferometers in the specific case of weak gravitational field when the Hamiltonian is at most quadratic in coordinates and conjugate momenta. A detailed discussion about Einstein and Fermi coordinates is presented in appendix. We apply the results in Sect. 3 to derive the phase shift signal for two specific atom interferometer configurations. Finally, in Sect. 4 we discuss possible experimental schemes and evaluate the sensitivity for the detection of gravitational waves.

2 The ABCD matrices for matter waves and phase-shift formula for atom interferometers

In this section we recall the ABCD formalism for matter waves and apply it to calculation of phase shift formula. The discussion is based on the relativistic Schroedinger-type equation for atom waves and its analysis in [26] and references therein.

2.1 The ABCD matrices for matter waves

In the following, we assume that the Hamiltonian relative to the motion of the center of mass is a quadratic polynomial of momentum and position operators,

as in most cases of relevance in AI:

$$H = \frac{1}{2M^*} \vec{p} \cdot \vec{\beta}(t) \cdot \vec{p} + \frac{1}{2} \vec{p} \cdot \vec{\alpha}(t) \cdot \vec{q} + \frac{1}{2} \vec{q} \cdot \vec{\delta}(t) \cdot \vec{p} - \frac{M^*}{2} \vec{q} \cdot \vec{\gamma}(t) \cdot \vec{q} + \vec{f}(t) \cdot \vec{p} - M^* \vec{g}(t) \cdot \vec{q} \quad (1)$$

where $\alpha, \beta, \gamma, \delta$ are suitable square matrices coefficients for the quadratic terms (with $\delta = -\tilde{\alpha}$, where the tilde indicates the transposed matrix); g is the gravity vector field and f is an external vector field. M^* is the relativistic mass ($M^* = M_0/\sqrt{1-v^2/c^2}$, where M_0 is the rest mass). The evolution of the wave packets by this Hamiltonian, via the Ehrenfest theorem, can be obtained through Hamilton's equations [26, 27]:

$$\frac{d\chi(t)}{dt} = \begin{pmatrix} \frac{dH}{dp} \\ -\frac{1}{M^*} \frac{dH}{dq} \end{pmatrix} = \Gamma(t)\chi(t) + \Phi(t) \quad (2)$$

where

$$\chi(t) = \begin{pmatrix} q \\ p/M^* \end{pmatrix} \quad \Phi(t) = \begin{pmatrix} f(t) \\ g(t) \end{pmatrix} \quad (3)$$

and

$$\Gamma(t) = \begin{pmatrix} \alpha(t) & \beta(t) \\ \gamma(t) & \delta(t) \end{pmatrix} \quad (4)$$

The integral of Hamilton's equations can be written through the ABCD matrices as

$$\chi(t) = \begin{pmatrix} A(t, t_0) & B(t, t_0) \\ C(t, t_0) & D(t, t_0) \end{pmatrix} \left[\chi(t_0) + \begin{pmatrix} \xi(t, t_0) \\ \psi(t, t_0) \end{pmatrix} \right] \quad (5)$$

where

$$\begin{pmatrix} \xi(t, t_0) \\ \psi(t, t_0) \end{pmatrix} = \int_{t_0}^t \mathcal{M}(t_0, t') \Phi(t') dt' \quad (6)$$

and

$$\mathcal{M}(t, t_0) = \begin{pmatrix} A(t, t_0) & B(t, t_0) \\ C(t, t_0) & D(t, t_0) \end{pmatrix} = \mathcal{T} \exp \int_{t_0}^t \Gamma(t') dt' \quad (7)$$

with \mathcal{T} the time ordering operator. A perturbative expansion leads to [27]:

$$\mathcal{M}(t, t_0) = 1 + \int_{t_0}^t \Gamma(t') dt' + \int_{t_0}^t dt' \int_{t_0}^{t'} \Gamma(t') \Gamma(t'') dt'' + \dots \quad (8)$$

The Eq. (7) can be used to find the ABCD matrices which determine the evolution of the wave packets in presence of the GW, h . If we consider the simple case in which the GW is the only (weak) field, in the two coordinate systems discussed in Appendix A, for a single Fourier component Ω we have up to the first order in $h(\Omega)$:

Fermi coordinates

$$\begin{aligned}\vec{\alpha} &= \vec{\delta} = 0 \\ \vec{\beta} &= \vec{1} \\ \vec{\gamma} &= \frac{\Omega^2}{2} \vec{h}\end{aligned}\tag{9}$$

$$\begin{aligned}A(t_2, t_1) &= 1 - \gamma(\Omega)e^{i\Omega t_1} \left[\frac{e^{i\Omega(t_2-t_1)} - 1}{\Omega^2} + \frac{t_2 - t_1}{i\Omega} \right] \\ B(t_2, t_1) &= (t_2 - t_1) + \\ &+ \frac{\gamma(\Omega)}{\Omega^2} e^{i\Omega t_1} \left[-(t_2 - t_1) \left(e^{i\Omega(t_2-t_1)} + 1 \right) + \frac{2(e^{i\Omega(t_2-t_1)} - 1)}{i\Omega} \right] \\ C(t_2, t_1) &= \gamma(\Omega)e^{i\Omega t_1} \left[\frac{e^{i\Omega(t_2-t_1)} - 1}{i\Omega} \right] \\ D(t_2, t_1) &= 1 + \gamma(\Omega)e^{i\Omega t_1} \left[\frac{(t_2 - t_1)e^{i\Omega(t_2-t_1)}}{i\Omega} + \frac{e^{i\Omega(t_2-t_1)} - 1}{\Omega^2} \right]\end{aligned}\tag{10}$$

where $\gamma(\Omega) = h(\Omega)\Omega^2/2$, $h(\Omega) = \int h(t) \exp(-i\Omega t) dt$, $i = \sqrt{-1}$.

Einstein coordinates

$$\begin{aligned}\vec{\alpha} &= \vec{\delta} = \vec{\gamma} = 0 \\ \vec{\beta} &= \vec{h}(t) - \vec{\eta}\end{aligned}\tag{11}$$

$$\begin{aligned}A(t_2, t_1) &= 1 \\ B(t_2, t_1) &= (t_2 - t_1) + \frac{h(\Omega)}{i\Omega} e^{i\Omega t_1} \left[e^{i\Omega(t_2-t_1)} - 1 \right] \\ C(t_2, t_1) &= 0 \\ D(t_2, t_1) &= 1\end{aligned}\tag{12}$$

where $\vec{\eta}$ is the Minkowskian matrix.

2.2 The phase shift formula for atom interferometers

The total phase difference between the two arms, s and i , of an atom interferometer can be expressed as the sum of three terms: the difference in the action integral along each path; the difference in the phases imprinted by the beam-splitters on the atom waves; the contribution from the splitting of the wave packets at the exit of the interferometer [26]:

$$\begin{aligned}\Delta\varphi = & \frac{1}{\hbar} \sum_{j=1}^N [S_s(t_{j+1}, t_j) - S_i(t_{j+1}, t_j)] + \\ & + \sum_{j=1}^N [(k_{sj}q_{sj} - k_{ij}q_{ij}) - (\omega_{sj} - \omega_{ij})t_j + (\vartheta_{sj} - \vartheta_{ij})] + \\ & + \frac{1}{\hbar} [p_{sD}(q - q_{sD}) - p_{iD}(q - q_{iD})]\end{aligned}\quad (13)$$

where $S_{sj} = S_s(t_{j+1}, t_j)$ and $S_{ij} = S_i(t_{j+1}, t_j)$ are the action integrals along s (i) path; $k_{sj}(k_{ij})$ is the momentum transferred to the atoms by the j -th beam-splitter along the s (i) arm; q_{sj} and q_{ij} are the coordinates of the beam splitter/atom interaction; $\omega_{sj}(\omega_{ij})$ is the angular frequency of the laser beam; $\vartheta_{sj}(\vartheta_{ij})$ is the phase of the laser beam at the j -th interaction with the atom; D is the exit port.

Assuming the same input point for the two arms and using the "mid point" property [7] in integrating over the space at the output, the phase shift difference $\Delta\varphi$ between the two arms (s, i) for an interferometer with N beam splitters can be written as:

$$\begin{aligned}\Delta\varphi = & \sum_{j=1}^N (k_{sj} - k_{ij}) \frac{q_{sj} + q_{ij}}{2} + \sum_{j=1}^N (\omega_{sj} - \omega_{ij}) t_j + \\ & + \sum_{j=1}^N (\vartheta_{sj} - \vartheta_{ij}) + \sum_{j=1}^N \frac{(M_{sj} - M_{ij})c^2}{\hbar} \tau_j\end{aligned}\quad (14)$$

where $M_{sj}(M_{ij})$ is the mass of the atom in the s (i) arm and τ_j is a proper time at the j -th interaction.

3 Phase calculation for different AI geometries

In this section, we use the ABCD formalism to find the resulting phase shift $\Delta\varphi$ for typical atom interferometer schemes [4]. The approach is in the frequency space of complex Fourier transform in order to describe both the amplitude and the phase of the resulting $\Delta\varphi$. We consider here the trapezoidal interferometer, first suggested in [28], and the parallelogram-shaped interferometer, both in Fermi and Einstein coordinates, retaining only terms up to the first order in \hbar .

3.1 Trapezoidal AI

The scheme of a trapezoidal interferometer is shown in Fig. 1. The interaction of the atom with two counter-propagating pairs of copropagating beams (BS1-BS4) gives rise to a trapezoidal-shaped closed circuit. By using Eq. (14), we obtain the expression of the phase shift for the two arms (s,i) of the interferometer:

$$\begin{aligned} \Delta\varphi = & k_1 q_1 + \frac{1}{2} k_{s2} (q_{s2,b} + q_{i2,a}) + \frac{1}{2} k_{s3} (q_{i3,a} + q_{s3,a}) + \frac{1}{2} k_4 (q_{s4,b} + q_{i4,a}) \\ & + 2(\Omega_L T - \Omega_{ba} \tau) + \vartheta_1 - \vartheta_2 + \vartheta_3 - \vartheta_4 \end{aligned} \quad (15)$$

where Ω_L is the laser frequency and Ω_{ba} is the frequency of the atomic transition involving ground (a) and excited (b) states; ϑ_i are the proper laser phases. Expressing all the q_j coordinates through the ABCD matrices, the phase difference $\Delta\varphi$ at the output of the interferometer is then given by:

$$\begin{aligned} \Delta\varphi = & k_1 q_1 [1 - 2A(T, 0) + A(2T, 0)] + \\ & + \frac{k_1}{2} [B(2T, 0) - 2B(T, 0)] \left(\frac{p_1}{M_b} + \frac{p_1}{M_a} + \frac{\hbar k_1}{M_b} \right) \\ & - k_1 B(2T, T) \frac{\hbar k_1}{M_b} + 2\Omega_L T - 2\Omega_{ba} \tau + \vartheta_1 - \vartheta_2 + \vartheta_3 - \vartheta_4 \end{aligned} \quad (16)$$

where M_a and M_b are the masses of the atom in the ground and excited state, respectively; the expression for the A, B, C, D matrices depends on the coordinate system.

Let's first consider Fermi coordinates. From Eq. (16) and Eq. (10), we obtain for the phase difference for this configuration

$$\begin{aligned} \Delta\varphi(\Omega) = & -\frac{\Omega \hbar(\Omega)}{2} \left(\frac{1}{M_a} + \frac{1}{M_b} \right) T^2 k_1 p_1 \cdot \\ & \cdot \left\{ \left[\sin \Omega T \left(\frac{\sin(\Omega T/2)}{\Omega T/2} \right)^2 + \frac{\cos 2\Omega T - \cos \Omega T}{\Omega T} \right] + \right. \\ & + i \left[\frac{\sin 2\Omega T - \sin \Omega T}{\Omega T} - \cos \Omega T \left(\frac{\sin(\Omega T/2)}{\Omega T/2} \right)^2 \right] \Big\} + \\ & + \hbar(\Omega) \frac{\hbar k_1^2 T}{M_b} \left[\left(1 - \frac{\sin \Omega T}{\Omega T} \right) \cos \Omega T + i \left(1 - \frac{\sin \Omega T}{\Omega T} \right) \sin \Omega T \right] + \\ & + \frac{\Omega^2 \hbar(\Omega)}{2} T^2 k_1 q_1 \left[\frac{\sin(\Omega T/2)}{\Omega T/2} \right]^2 (\cos \Omega T + i \sin \Omega T) + \\ & + 2 \left(\Omega_L - \frac{\hbar k_1^2}{2M_b} \right) T - 2\Omega_{ba} \tau + \vartheta_{1F} - \vartheta_{2F} + \vartheta_{3F} - \vartheta_{4F} \end{aligned} \quad (17)$$

Considering Einstein coordinates, from Eq. (16) and Eq. (12), we obtain

$$\begin{aligned}
\Delta\varphi(\Omega) = & -\frac{\Omega h(\Omega)}{2} \left(\frac{1}{M_a} + \frac{1}{M_b} \right) T^2 k_1 p_1 \cdot \\
& \cdot \left[\sin \Omega T \left(\frac{\sin(\Omega T/2)}{\Omega T/2} \right)^2 - i \cos \Omega T \left(\frac{\sin(\Omega T/2)}{\Omega T/2} \right)^2 \right] + \\
& -\frac{\hbar k_1^2 T}{M_b} h(\Omega) \left(\cos \Omega T \frac{\sin \Omega T}{\Omega T} + i \sin \Omega T \frac{\sin \Omega T}{\Omega T} \right) + \\
& + 2 \left(\Omega_L - \frac{\hbar k_1^2}{2M_b} \right) T - 2\Omega_{ba}\tau + \vartheta_{1E} - \vartheta_{2E} + \vartheta_{3E} - \vartheta_{4E}
\end{aligned} \tag{18}$$

where ϑ_{iE} are the laser phases in the Einstein coordinates system. They are different because in Einstein coordinates the index of refraction for the vacuum is varying with $h(t)$ or, which is the same, we have an extra (Fourier transformed) contribution $\delta k \cong k[h(t, \Omega)/2]\exp(i\Omega t)$ to the momentum transferred at the beam-splitter positions as a consequence of the apparent photon velocity $v \cong c[1 + (h/2)]$. This can be accounted for in the phase terms leading to an extra term $-\delta k(t, \Omega)$ in Eq. (15), as in spatial beam-splitters [26]. By inserting these laser phases and using the coordinates transformation rules in GR between the two systems here considered (see Appendix B), the resulting phase shift difference is coincident with the one obtained in Fermi coordinates, as expected for a scalar quantity which is a physical result in spite of different descriptions.

3.2 Parallelogram-shaped AI

The scheme of a parallelogram-shaped AI is shown in Fig. 2. In this case, the interaction of the atom with four copropagating laser beams gives rise to a parallelogram-shaped closed circuit.

The phase difference at the output of this interferometer is given by:

$$\begin{aligned}
\Delta\varphi = & k_1 q_1 [1 - 2A(T, 0) + A(2T, 0)] + \\
& + \frac{k_1}{2} [B(2T, 0) - 2B(T, 0)] \left(\frac{p_1}{M_a} + \frac{p_1}{M_b} + \frac{\hbar k_1}{M_b} \right) + \\
& + \frac{\hbar k_1^2}{2M_b} B(2T, T) [D(T, 0) - 1] \epsilon + \vartheta_1 - \vartheta_2 - \vartheta_3 + \vartheta_4
\end{aligned} \tag{19}$$

up to the first order in ϵ , where $\epsilon = (M_b - M_a)/M_a$. The only difference from the case of a trapezoidal interferometer (Eq. (16)) is in the recoil term, which is proportional to the relative energy difference between ground and excited states. Using Fermi coordinates, from Eq. (10) we obtain:

$$\Delta\varphi(\Omega) = -\frac{\Omega h(\Omega)}{2} T^2 k_1 \left(\frac{p_1}{M_a} + \frac{p_1}{M_b} + \frac{\hbar k_1}{M_b} \right).$$

$$\begin{aligned}
& \cdot \left\{ \left[\sin \Omega T \left(\frac{\sin(\Omega T/2)}{\Omega T/2} \right)^2 + \frac{\cos 2\Omega T - \cos \Omega T}{\Omega T} \right] + \right. \\
& + i \left[\frac{\sin 2\Omega T - \sin \Omega T}{\Omega T} - \cos \Omega T \left(\frac{\sin(\Omega T/2)}{\Omega T/2} \right)^2 \right] \Big\} + \\
& + \frac{\Omega^2 h(\Omega)}{2} T^2 k_1 q_1 \left(\frac{\sin(\Omega T/2)}{\Omega T/2} \right)^2 (\cos \Omega T + i \sin \Omega T) + \\
& + \frac{\epsilon}{2} \frac{\hbar k_1^2}{2M_b} h(\Omega) T^2 \left[\left(\sin \Omega T - \frac{1 - \cos \Omega T}{\Omega T} \right) + i \left(\frac{\sin \Omega T}{\Omega T} - \cos \Omega T \right) \right] + \\
& + \vartheta_{1F} - \vartheta_{2F} - \vartheta_{3F} + \vartheta_{4F}
\end{aligned} \tag{20}$$

Considering Einstein coordinates, we obtain:

$$\begin{aligned}
\Delta\varphi(\Omega) = & -\frac{\Omega h(\Omega)}{2} T^2 k_1 \left(\frac{p_1}{M_a} + \frac{p_1}{M_b} + \frac{\hbar k_1}{M_b} \right) \cdot \\
& \cdot \left[\sin \Omega T \left(\frac{\sin(\Omega T/2)}{\Omega T/2} \right)^2 - i \cos \Omega T \left(\frac{\sin(\Omega T/2)}{\Omega T/2} \right)^2 \right] + \\
& + \vartheta_{1E} - \vartheta_{2E} - \vartheta_{3E} + \vartheta_{4E}
\end{aligned} \tag{21}$$

The same considerations of paragraph 3.1 apply in this case about the identity of the results in the two descriptions.

4 Possible schemes and expected sensitivities

The results in previous section provide the phase shift at the output of the atom interferometer induced by a gravitational wave with amplitude h and frequency Ω for the typical schemes considered. In order to determine the sensitivity of the interferometer, that is the minimum detectable amplitude $h(\Omega)$, we assume shot-noise-limited detection of the atoms, corresponding to a phase noise given by $\Delta\varphi(\Omega) = \eta/\sqrt{\dot{N}}$ where η is a detection efficiency and \dot{N} is the atoms flow at the detector. The resulting sensitivity $h(\Omega)$ (at S/N ratio equal 1) can be written as

$$h(\Omega) = \frac{\eta}{\sqrt{\dot{N}}} \frac{1}{f(\Omega)\Sigma} \tag{22}$$

where Σ is a scale factor and $f(\Omega)$ is the resonance function of the interferometer. Neglecting the clock and recoil terms, from Eq. (17) we obtain:

$$h(\Omega) = \frac{\eta \hbar}{p_T L \sqrt{\dot{N}}} \frac{1}{f(\Omega)} \tag{23}$$

where L is the characteristic linear dimension of the interferometer, $p_T = mv_T$ with v_T the transversal velocity acquired by the atoms in the splitting process and $2/m = 1/M_a + 1/M_b$, and where

$$f(\Omega) = \Omega T \left\{ \left[\sin(\Omega T) \left(\frac{\sin(\Omega T)/2}{\Omega T/2} \right)^2 + \frac{\cos(2\Omega T) - \cos(\Omega T)}{\Omega T} \right] + \right. \\ \left. + i \left[\frac{\sin(2\Omega T) - \sin(\Omega T)}{\Omega T} - \cos(\Omega T) \left(\frac{\sin(\Omega T)/2}{\Omega T/2} \right)^2 \right] \right\} \quad (24)$$

From Eq. (23), it is evident that in order to achieve the required sensitivity while keeping a sufficiently large detection bandwidth it is necessary to realize large values of L and p_T .

In order to evaluate the performance of these new detectors for GWs, we analyzed a few specific cases. It is important to notice that in this analysis we did not treat other noise sources that, as in optical GW detectors, can affect the performance of the AI detector. Examples are the suspension of optics required for the manipulation of the laser beams or the phase noise of the laser itself. Based on the work for optical GW detectors and progress in ultrastable lasers for future optical clocks, suitable laser sources and suspension systems can be envisaged. A detailed analysis of the overall noise budget, including technological aspects, is beyond the scope of the present paper.

Let us consider first an atom interferometer based on a fast beam of hydrogen atoms. If we take $T = 10^{-3}$ s and a length $L = 10^3$ m, similar to present optical interferometers detectors, we have $v_L = 10^6$ m/s. As shown in Fig.3, in this case a sensitivity $h(\Omega)$ of about $10^{-21}/Hz^{1/2}$ is achieved for $v_T \approx 10$ m/s with a flux of 10^{18} atoms/s in the atomic beam [29]. The recoil velocity for a hydrogen atom absorbing a $Ly - \alpha$ photon is $v_{rec} = 3.3$ m/s. Although the absorption of a photon followed by spontaneous emission destroys coherence and cannot be used to deflect atomic trajectories in an interferometer, it is conceivable to use two-photon Raman transitions between the two hyperfine levels of H ground state. A single Raman pulse transfers a velocity $v_T = 2v_{rec}$. Raman transitions have already been used in AI based on alkali atoms [4] and the possibility to use multiple Raman pulses sequences to increase the enclosed area and the resulting sensitivity was also demonstrated [30]. A practical limitation at present would be the required power (≈ 10 W) of laser radiation at the $Ly\alpha$ wavelength. This is orders of magnitude larger than what can be presently achieved as cw radiation [31] but closer to what is produced in pulsed mode [32]. An alternative scheme is the excitation of a two-photon transition from the ground state to long lived excited states [33, 34]. A large recoil can be transferred by combining $1s - 2s$ excitation with optical transitions from the $2s$ state to high lying p states [35]. Such a scheme is also compatible with a ground based apparatus because of the negligible vertical displacement of the atomic beam during the

short total time of flight. Other cases we considered for fast beams of heavier atoms do not meet the requirements for the scheme we considered because of the difficulty to transfer a large enough transverse momentum to the atoms while keeping T small enough in order to keep a large bandwidth. An improvement in sensitivity, at the expense of a reduced bandwidth, could be achieved by increasing T and correspondingly the linear dimensions of the interferometer. In this case, however, a gravity-free apparatus in space should be considered (Fig.3).

A different case we considered is an interferometer based on cold atoms. In this case, it is more useful to rewrite Eq. (23) in the form:

$$h(\Omega) = \frac{\eta \hbar}{\sqrt{N}} \left(\frac{p_L}{p_T} \right) \frac{T}{mL^2} \frac{1}{f(\Omega)} \quad (25)$$

where m is the atomic mass. It is apparent that in this scheme, by relaxing the constraint on T , the sensitivity is better the larger is the value of m and the smaller is p_L . As an example, if $v_L = 1 \text{ m/s} = 2v_T$, $L = 50 \text{ m}$ and $m \approx 10^2 \text{ a.m.u.}$, a sensitivity of about $10^{-21}/Hz^{1/2}$ results at frequencies around 10 mHz (Fig. 3). The long time of flight $T \approx 50 \text{ s}$, for which a gravity-free scheme would be required, leads of course to a narrower bandwidth.

5 Conclusions

We investigated the possibility of detecting gravitational waves using atom interferometers based on light fields as beam-splitters. The phase shift at the output of the interferometers was calculated for presently known schemes using both Einstein and Fermi coordinates. Considering sensitivities of the same order of magnitude as the ones of present optical gravitational wave detectors, we estimated the resulting values for relevant parameters. The results show that dedicated technological developments would be needed to achieve the required values which are beyond those presently available. New schemes for atom interferometers, beam splitters, and high flux coherent atomic sources can lead to an increase in sensitivity and make atom interferometers competitive with other gravitational wave detectors.

Acknowledgments

The authors acknowledge useful discussions with Ch. J. Bordé.

Appendix A: Einstein vs Fermi coordinates

In general relativity (GR) all the coordinates systems are *a priori* equivalent. The predicted physical results do not depend on the specific coordinates system although different descriptions depend on coordinates systems. Generally speaking, a change of coordinates is defined by any set of functions

$$x^\alpha = x^\alpha(y^\beta) \longleftrightarrow y^\alpha = y^\alpha(x^\beta) \quad \alpha, \beta = 0, 1, 2, 3 \quad (26)$$

where the invertibility is guaranteed if and only if

$$\det \left(\frac{\partial x^\alpha}{\partial y^\beta} \right) \neq 0 \quad (27)$$

In the following, we refer to the case in which deviations from the Minkowsky space of special relativity are due only to GWs in the weak field approximation, that is

$$g_{\mu\nu}(x) = \eta_{\mu\nu} + h_{\mu\nu}(x) \quad (28)$$

with $|h_{\mu\nu}| \ll 1$. We assume that no other field is present. In this case, the linearized Einstein field equations admit a plane wave solution for $h_{\mu\nu}$. It is always possible to choose Gaussian synchronous coordinates [36] in which

$$g_{0\mu} = g_{\mu 0} = (1, 0, 0, 0) \quad (29)$$

Let's choose the particular coordinates system in which two particles A and B, at rest in Minkowsky system, remain at rest even in presence of a GW. These are called Einstein coordinates (EC) and the related metrics can be written as

$$ds^2 = c^2 dt^2 - (1 - h_+) dx^2 - (1 + h_+) dy^2 - dz^2 + 2h_\times dx dy \quad (30)$$

for a wave propagating along the z axis; $h_+ = h_+(ct - z)$ and $h_\times = h_\times(ct - z)$ are the amplitudes of the two polarizations states. The world-lines of a free particle are geodesics [37]. It is important to note that the proper distance between two particles A and B always at rest in this system is varying with the amplitude of the GW [38]:

$$d^2 = d_0^2 + h_{ij}(t)(x_B^i - x_A^i)(x_B^j - x_A^j) \quad (31)$$

where $d_0^2 = (x_B^i - x_A^i)(x_B^i - x_A^i)$ in the hypothesis that the particles A and B are close enough to consider h_{ij} depending only on t. From another point of view, we can say that the flight time of a photon from A to B and back is varying, or that we have an index of refraction of the vacuum which is varying with the perturbation $h_{ij}(t)$.

The Einstein coordinates are formally the most convenient to describe plane GWs; they can be considered as a "wave system (TT gauge)". This is not an intuitive system, however, for measurements in a laboratory; as an extension

of "classical" approach, indeed, we search for inertial systems in which it is possible to preserve the Newtonian idea of "rigid stick" and related measurement method. Fermi coordinates (FC) are the best approximation to such a "Galilean system" [37, 39]. We choose a "fiducial observer" (free falling observer) at rest in the origin; the system is related to the geodesic line $x = y = z = 0$. This is a Minkowskian system if we disregard small terms as h_+ and h_\times [40]. The spatial axis are built as locally orthogonal coordinate lines whose direction can be checked by gyroscopes [39, 38, 40]. The transformation between the two systems EC and FC are [38, 40]:

$$\begin{aligned} X &= x - \frac{1}{2}h_+x + \frac{1}{2}h_\times y \\ Y &= y + \frac{1}{2}h_+y + \frac{1}{2}h_\times x \\ Z &= z + \frac{1}{4c}\dot{h}_+(x^2 - y^2) + \frac{1}{2c}\dot{h}_\times xy \\ T &= t + \frac{1}{4c^2}\dot{h}_+(x^2 - y^2) + \frac{1}{2c^2}\dot{h}_\times xy \end{aligned} \quad (32)$$

where X, Y, Z, T are Fermi coordinates, x, y, z, t are Einstein coordinates, and the dot indicates the time derivative.

Two particles A and B , initially at rest in FC, move approximately as

$$\begin{aligned} X_{A,B} &= x_{A,B} - \frac{1}{2}h_+x_{A,B} + \frac{1}{2}h_\times y_{A,B} \\ Y_{A,B} &= y_{A,B} + \frac{1}{2}h_+y_{A,B} + \frac{1}{2}h_\times x_{A,B} \\ Z_{A,B} &= z_{A,B} \end{aligned} \quad (33)$$

In this case, the proper distance does not change while the distance between the two particles does: the index of refraction of the vacuum is 1. Time of flight of a photon between two test masses A and B is the same in both systems: it is a physical result, indeed, in spite of the different descriptions.

It is to be noted that the particle A moves with respect to the particle B as subjected to the "tidal" force $F_{A,i} = \frac{1}{2}m_A x^j \frac{d^2 h_{ji}}{dt^2}$.

From Eq. (32), it appears that in the study of interaction of GW with experimental devices, Einstein coordinates are not the most suitable because of the very complex motion resulting for an observer in the laboratory frame; Fermi coordinates can indeed be considered as the natural extension of a "Cartesian inertial system" of the local observer [41, 42, 43].

Appendix B: Gauge invariance

Demonstrating the invariance of the results in Sect. 3 under general gauge transformations is the subject of ongoing work; here we restrict the discussion to the

so called "long wavelength approximation" [42, 43].

It is easy to see that the transformation matrix S from EC to FC of Appendix A behaves as

$$S = I + O(h) \quad (34)$$

where I is the identity matrix; furthermore from Eq.32, we get

$$T = t + O(hL^2/c\lambda) \quad (35)$$

From Eq.34, using Eq.35 in the approximation $L/\lambda \rightarrow 0$ after the insertion of the δk term for proper laser phases, the identity of results in both coordinates systems used in Sect.3 follows.

It is worth noting that, starting from general FC, it is possible to build a simpler "laboratory frame", that is a *rigid coordinates system* [23, 40], which preserves the FC properties in the hypothesis of constant z (wavefront of the gravitational plane wave) near the $Z = 0$ plane (the plane of the interferometer) [25, 40, 44]. Considering for simplicity only the $+$ polarization, the transformation law from the EC with metric

$$ds^2 = c^2 dt^2 - (1 - h_+) dx^2 - (1 + h_+) dy^2 - dz^2 \quad (36)$$

to the rigid system, is

$$\begin{aligned} t &= T \\ x &= X + \frac{1}{2} h_+ X \\ y &= Y - \frac{1}{2} h_+ Y \\ z &= Z \end{aligned} \quad (37)$$

with transformation matrix

$$\begin{pmatrix} 1 & 0 & 0 & 0 \\ \frac{1}{2c} \dot{h}_+ X & 1 + \frac{1}{2} h_+ & 0 & -\frac{1}{2c} \dot{h}_+ X \\ -\frac{1}{2c} \dot{h}_+ Y & 0 & 1 - \frac{1}{2} h_+ & \frac{1}{2c} \dot{h}_+ Y \\ 0 & 0 & 0 & 1 \end{pmatrix} \quad (38)$$

and metric

$$\begin{aligned} ds^2 &= c^2 dT^2 - dX^2 - dY^2 - dZ^2 + \\ &+ \frac{\dot{h}_+}{c} (X dX dZ - Y dY dZ - cX dX dT + cY dY dT) \end{aligned} \quad (39)$$

Writing proper ABCD matrices for the rigid coordinates system by using Eq. 39, the same results as in Eq. 17 or Eq. 20 can be obtained, thus demonstrating the identity of the results in rigid, Fermi, and Einstein coordinates systems.

References

- [1] For an introduction, see e.g. : P.R. Saulson, *Fundamental of Interferometric GW detectors*, World Scientific, Singapore (1994)
- [2] For a general update see the following special issue: Classical and Quantum Gravity, 23 (2006)
- [3] For LISA project, see the special issue: Classical and Quantum Gravity, 22, (2005)
- [4] P. Berman (Ed.), *Atom Interferometry*, Academic Press, N.Y. (1997)
- [5] S. Chu, in *Coherent atomic matter waves*, LXXII Les Houches Session, R. Kaiser, C. Westbrook, F. David (Eds.), Springer Verlag, N.Y. (2001)
- [6] A. Peters, K.Y. Chung, S. Chu, Metrologia, 38, 25-61 (2001)
- [7] Ch. J. Bordé, Metrologia, 39, 435-463 (2002)
- [8] A. Peters, K.Y. Chung, S. Chu, Nature, 400, 849-852 (1999)
- [9] J.M. McGuirk, G.T. Foster, J.B. Fixler, M.J. Snadden, M.A. Kasevich, Phys. Rev. A, 65, 33608 (2002)
- [10] T.L. Gustafson, A. Landragin, M.A. Kasevich, Class. Quantum Grav. 17, 2385-2398 (2000)
- [11] G.E. Stedman, Rep. Prog. Phys., 60, 615-688 (1997)
- [12] A. Bertoldi, G. Lamporesi, L. Cacciapuoti, M. de Angelis, M. Fattori, T. Petelski, A. Peters, M. Prevedelli, J. Stuhler, G.M. Tino, Eur. Phys. J. D 40, 271-279 (2006)
- [13] J. B. Fixler, G. T. Foster, J. M. McGuirk, M. A. Kasevich, Science 315, 74-77 (2007)
- [14] S. Dimopoulos, P.W. Graham, J.M. Hogan, M.A. Kasevich, gr-qc/0610047
- [15] HYPER, Assessment Study Report, ESA-SCI (2000), 10 , July 2000; C. Jentsch, T. Müller, E. M. Rasel, and W. Ertmer, Gen. Rel. Grav. 36, 2197-2221 (2004).
- [16] G. Ferrari, N. Poli, F. Sorrentino, G. M. Tino, Phys. Rev. Lett. 97, 060402 (2006), and references therein.
- [17] B. Linet, P. Tourrenc, Can. J. Phys., 54, 1129-1133 (1976)
- [18] L. Stodolsky, GRG, 11, 391-405 (1979)

- [19] J. Anandan, R.Y. Chiao, Gen. Rel. Grav. 14, 515-521 (1982)
- [20] Ch. J. Bordé, J. Sharma, Ph. Tournenc, and Th. Damour, J. Physique L-983, 44 (1983)
- [21] Preliminary results of this work were presented by one of the authors at *2004 Aspen Winter Conference on Gravitational Waves and their Detection*, Aspen, February 2004 (http://www.ligo.caltech.edu/LIGO_web/Aspen2004/pdf/vetrano.pdf)
- [22] R.Y. Chiao, A.D. Speliotopoulos, J. Mod. Opt. 51, 861 (2004)
- [23] A. Roura, D.R. Brill, B.L. Hu, C.W. Misner, W.D. Phillips, Phys. Rev. D 73, 084018 (2006)
- [24] S. Foffa, A. Gasparini, M. Papucci, R. Sturani, Phys. Rev. D 73, 022001 (2006)
- [25] P. Delva, M.-C. Angonin, P. Tournenc, Phys. Lett. A 357, 249-254 (2006)
- [26] Ch. J. Bordé, Gen. Rel. Grav. 36, 475-501 (2004)
- [27] C. Antoine, Ch. J. Bordé, J. Opt. B : Quantum Semiclass. Opt., 5, 199-207 (2003)
- [28] Ch. J. Bordé, Phys. Lett. A 140, 10-12 (1989)
- [29] G. Scoles Ed., Atomic and Molecular Beam Methods, Oxford Un. Press, New York (1988)
- [30] J.M. McGuirk, M.J. Snadden, M.A. Kasevich, Phys. Rev. Lett. 85, 4498 (2000)
- [31] K.S.E. Eikema, J. Walz, T.W. Hänsch, Phys. Rev. Lett. 83, 3828 (1999)
- [32] I.D. Setija et al., Phys. Rev. Lett. 70, 2257 (1993)
- [33] B. Gross, A. Huber, M. Niering, M. Weitz, T.W. Hänsch, Europhys. Lett. 44, 186 (1998)
- [34] T.W. Hijmans, P.W.H. Pinkse, A.P. Mosk, M. Weidmuller, M.W. Reynolds, J.T.M. Walraven, C. Zimmerman, Hyperf. Interact. 127, 175 (2000)
- [35] T. Heupel, M. Mei, M. Niering, B. Gross, M. Weitz, T.W. Hänsch, Ch.J. Bordé, Europhys. Lett. 57, 158 (2002)
- [36] H. Stephani, *General Relativity*, Cambridge University Press, 2nd Edition, New York (1990)

- [37] C.W. Misner, K.S. Thorne, A. Wheeler, *Gravitation*, Freeman and Co, S.Francisco (1973)
- [38] A. Brillet, T. Damour, Ph. Tourrenc, Ann. Phys. Fr. 10, 201-218 (1985)
- [39] F.K. Manasse, C.W. Misner, J. Math. Phys. 4, 735-745 (1963)
- [40] L.P. Grishchuk and A.G. Polnarev, in *General Relativity and Gravitation*, A. Held Ed., Vol. 2, Plenum press, New York (1981)
- [41] P.L. Fortini, C. Gualdi, Nuovo Cim. 71 B, 37-54 (1982)
- [42] G. Flores, M. Orlandini, Nuovo Cim. 91 B, 236-240 (1986)
- [43] V. Faraoni, Nuovo Cim. 107 B, 631-642 (1992)
- [44] D. Baskaran, L.P. Grishchuk, Class. Quant. Grav. 21, 4041-4061 (2004)

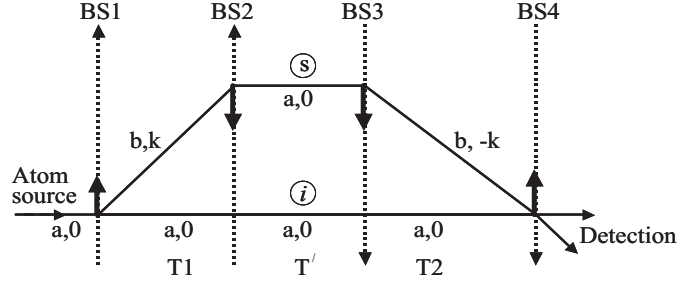


Figure 1: Scheme of the trapezoidal interferometer. Dotted arrows represent laser beams acting as beam-splitters (BS1-BS4); bold continuous arrows show the relevant momentum transferred to the atom; a: ground internal atomic state; b: excited internal atomic state; \mathbf{k} : transferred momentum (in \hbar units). In the text $T_1 = T_2 = T$ and $T' \rightarrow 0$.

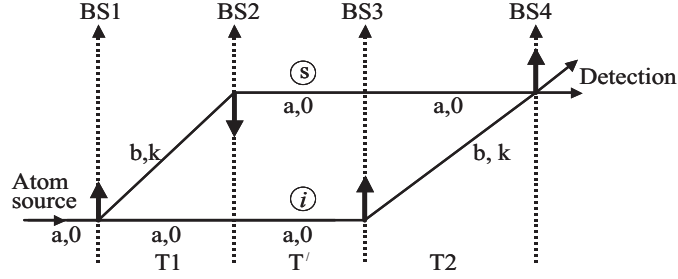


Figure 2: Scheme of a parallelogram interferometer. Dotted arrows represent laser beams acting as beam-splitters (BS1-BS4); bold continuous arrows show the relevant momentum transferred to the atom; a: ground internal atomic state; b: excited internal atomic state; \mathbf{k} : transferred momentum (in \hbar units). In the text $T_1 = T_2 = T$ and $T' \rightarrow 0$.

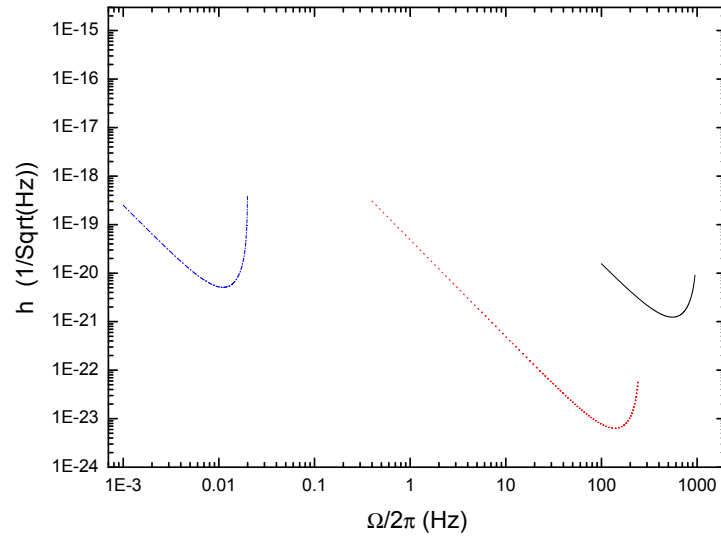


Figure 3: Sensitivity curves of GW detectors based on atom interferometry for the three parameter sets discussed in the text: $L = 10^3$ m, $v_L = 10^6$ m/s (continuous line); $L = 2 \cdot 10^5$ m, $v_L = 5 \cdot 10^7$ m/s (dotted line); $L = 50$ m, $v_L = 1$ m/s (dashed-dotted line).